ELSEVIER

Chemical Physics 275 (2002) 333–354

Chemical Physics

www.elsevier.com/locate/chemphys

Theory of linear absorption spectra of biological and non-biological chromophore complexes

J. Schütze[a], B. Brüggemann[a], Th. Renger[b,*], V. May[a]

[a] *Institut für Physik, Humboldt-Universität zu Berlin, Hausvogteiplatz 5-7, D-10117 Berlin, Germany*
[b] *A.A. Noyes Laboratory of Chemical Physics, California Institute of Technology, 127-72 Caltech, Pasadena, CA 91125, USA*

Received 11 June 2001

Abstract

Linear frequency-domain absorption spectra of chromophore complexes are studied within a Frenkel-exciton model including static and dynamic disorder. While static disorder is accounted for by explicite numerical ensemble averaging, dynamic disorder is described via the coupling of excitons to low-frequency vibrational modes (solvent or protein modes) and to high-frequency (intra-molecular) modes. Using a time-dependent formulation of the absorption density matrix theory can be applied. It is shown that the non-Markovian version of the Quantum Master Equation offers a certain approximation for the absorption based on a partial summation with respect to the exciton–vibrational coupling. In a first application the approach is used to describe absorption spectra of phenylacetylene dendrimers where static disorder is introduced to account for solvent induced deviations from the ideal structure. A detailed analysis of the long-wavelength tail underlines the dominance of structure fluctuations in the outer part of the dendrimer. While a concrete classification of the low-frequency modes remains impossible (according to the presence of static disorder) a qualitative estimate of the high-frequency modes becomes feasible. In a second application linear absorption of the photosynthetic antenna complex LHC-II of higher plants is analyzed and different structural parameters (Huang Rhys factor, inhomogeneous width of site energies, exciton state life times) are deduced. In particular the measured temperature dependence of the absorption spectrum can be well reproduced. A simultaneous fit of the circular dichroism spectrum at 77 K is used to discriminate between two different structural models.

1. Introduction

The detection of linear absorption spectra related to molecular system represents a standard technique of optical spectroscopy. Of course, as discussed before (see, e.g. [1]), it only gives a restricted amount of information, the reason being to a large part the presence of inhomogeneous broadening. To overcome this difficulty often more involved techniques come to an application. To remove the influence of inhomogeneous broadening hole burning or fluorescence line-narrowing spectroscopy can be used if the lowest exciton state shall be investigated. If, however, the relaxation of excitons between different electronic states is of interest time-resolved non-linear optical spectroscopy is the choice. In general, non-linear tech-

* Corresponding author.

0301-0104/02/$ - see front matter
PII: S0301-0104(01)00539-0

niques must be used if excited state absorption shall be investigated. Single molecule spectroscopy may also be used to remove part of the static disorder, however, slow conformational motion will still be a broadening factor in the spectrum since it is obtained as a time average over many optical cycles of a single molecule.

But, continuous wave (cw) linear absorption spectroscopy never lost its importance as a simple technique to give reference data for all these more difficult approaches. Furthermore, if the system that shall be studied is not so well structurally characterized a simple technique often has its advantage, because it allows for a more general interpretation than more involved techniques.

For the following discussion we will denote the frequency dependent absorption according to

$$\alpha(\omega) = \frac{4\pi\omega n_{\mathrm{CC}}}{\hbar c} I(\omega), \tag{1}$$

where n is the volume density of the absorbing units, e.g. single chromophores or chromophore complexes (CC). The quantity $I(\omega)$ denotes the real part of the half-sided Fourier-transform of the dipole–dipole correlation function

$$C_{\mathrm{d-d}}(t) = \mathrm{tr}\{\hat{W}_{\mathrm{eq}}[\hat{\mu}(t), \hat{\mu}(0)]\}. \tag{2}$$

The expression contains the equilibrium statistical operator $\hat{W}_{\mathrm{eq}}$ of the considered system and the dipole operator $\hat{\mu}(t)$ for which time-dependence is given by the system Hamiltonian (without the coupling to the light-field). Note that $C_{\mathrm{d-d}}$ is a scalar since the dipole operators are multiplied according to a scalar product. Neglecting the so-called anti-resonant part, i.e., setting $C_{\mathrm{d-d}}(t) = \mathrm{tr}\{\hat{W}_{\mathrm{eq}}\hat{\mu}(t)\hat{\mu}(0)\}$ the simple sum-rule for the absorption $\int \mathrm{d}\omega\alpha(\omega)/2\pi\omega = 2\pi n\,\mathrm{tr}\{\hat{W}_{\mathrm{eq}}\hat{\mu}^2\}/\hbar c$ can be deduced. Inhomogeneous broadening can be accounted for by an averaging with respect to the different disordered configurations (labeled by $\langle\cdots\rangle_{\mathrm{dis}}$ in the following).

In simulating the optical absorption of dye aggregates or CC one is confronted with the interplay of two distinct interactions, the coupling of electronic excitations to vibrational degrees of freedom (vibrational DOF) and the interaction among the electronic excitations. An exact formula for the absorption can be given in the limit of vanishing electronic inter-chromophore coupling. And, additionally, it is necessary that the two electronic states involved in the absorption process of a single chromophore are characterized by potential energy surfaces (PESs) of the independent harmonic oscillator type (see, e.g. [1,2]). One obtains

$$I(\omega) = |\mathbf{d}|^2 \mathrm{e}^{-s(0)}\ \mathrm{Re}\int_0^\infty \mathrm{d}t \exp(\mathrm{i}(\omega - \omega_{\mathrm{eg}}) + s(t)), \tag{3}$$

where ω_{eg} denotes the intra-chromophore transition frequency and $\mathbf{d}$ is the related transition matrix element. The standard line-shape function has the form

$$s(t) = \int \mathrm{d}\omega\, \mathrm{e}^{-\mathrm{i}\omega t}(1 + n(\omega))(J(\omega) - J(-\omega)), \tag{4}$$

where the so-called spectral density $J(\omega)$ describes the electron–vibrational coupling upon the electronic transition. The great advantage of Eq. (3) is given by the fact that it can account for a huge (macroscopic) number of vibrational DOF. Once $J(\omega)$ is known all details of the absorption spectra can be calculated.

The other tractable case of a CC absorption spectrum is reached if one considers a set of chromophores coupled, e.g., via an electronic dipole–dipole interaction but being free of any influence of the vibrational degrees of freedom. In this case one may introduce delocalized excitations of the Frenkel-exciton type. The optical transition takes place into these states and we have

$$I(\omega) = \sum_\alpha |\mathbf{d}_\alpha|^2 \delta(\omega - \Omega_\alpha). \tag{5}$$

The quantity $\mathbf{d}_\alpha$ is the dipole matrix element for the transition into the (single) exciton state $|\alpha\rangle$ with energy $\hbar\Omega_\alpha$. Since larger absorbing units (the CC) are introduced, n in Eq. (1) has to be replaced by n_{CC} denoting the volume density of the CC.

After the early works on molecular excitons (see, e.g. [3–5]) it has been the subject of numerous theoretical considerations published within the last two decades (see, e.g. [6–9]) to combine both types of interactions and to find proper approximations for the various special cases of CC absorption

spectra. The problem never lost its attraction and was in the focus of theoretical activities in the late nineties, too (see, e.g. [10–15]). In particular, a number of papers concentrated on photosynthetic antenna systems (e.g. [16–18], see also the overviews in [19,20]).

It is the aim of the present contribution to present a further study of CC absorption, and in this manner, to interrelate formulas (3) and (5). This should enable one to obtain a proper approximation for CC where the inter-chromophore coupling as well as the exciton–vibrational coupling have to be considered at the same time (the interchromophore interaction is assumed strong enough to use the delocalized representation of Frenkel excitons). Our approach is based on the density matrix description of exciton motion formulated in the framework of the Quantum Master Equation (QME) for exciton states (see the recent overview [20]). If the non-Markovian version of the QME is used a formula for the absorption can be derived which accounts for both mentioned coupling mechanisms beyond any perturbation theory. This will be demonstrated in Section 3. The used Frenkel-exciton model is shortly introduced in Section 2, whereas the basics of density matrix theory are reviewed in Appendix C. Alternative approaches to determine the absorption in carrying out an expansion leading to vibrational satellites of increasing order are given in Appendices A and B.

The whole approach is applied in Section 4 to interpret spectra of phenylacetylene dendrimers measured in [21]. Chlorophyll–protein complexes in the photosynthetic apparatus of higher plants (light harvesting complex of photosystem two, LHC-II) are discussed in Section 5 as a second example of CC.

2. The exciton model of chromophore complexes

For notational convenience we shortly remind of the assumptions necessary to derive the Frenkel-exciton model for CC excitations including the coupling to different types of vibrational DOF. Since we are exclusively interested in the study of linear optical properties we will describe our CC by the Hamiltonian

$$H_{\mathrm{CC}} = H_0 + H_1, \tag{6}$$

which only incorporates a part related to the electronic ground-state and a part related to the first excited electronic state. The Hamiltonian

$$H_0 \equiv H_{\mathrm{vib}} = H_{\mathrm{lf}} + H_{\mathrm{hf}} \tag{7}$$

refers to the electronic ground-state $|0\rangle$ (where the electronic ground-state energy E_0 has been set equal to zero) and governs the dynamics of the various vibrational modes. We will provide two distinct classes, low-frequency mainly solvent vibrations described by H_{lf} and high-frequency intramolecular vibrations with Hamiltonian H_{hf}. The latter class will be handled in such a manner that vibrational satellites can appear in the optical spectra. The other class should be responsible for homogeneous line-broadening. This separation should be also understood as a separation into vibrational DOF which weakly couple to the electronic excitations (low-frequency vibrations) and those with a large coupling-strength (high-frequency vibrations). This identification has been done from a practical viewpoint by classifying different approximations but does not have any microscopic reason. Whenever this separation is not necessary we use the notation H_{vib} for the complete vibrational Hamiltonian.

The excited state part H_1 of Hamiltonian Eq. (6) is given by

$$H_1 = H_{\mathrm{ex}} + H_{\mathrm{ex\text{–}vib}} + H_{\mathrm{vib}} \tag{8}$$

with the standard Frenkel-exciton Hamiltonian H_{ex} and the coupling to the vibrational modes $H_{\mathrm{ex\text{–}vib}}$. The part H_{ex} may be either written in the site representation

$$H_{\mathrm{ex}} = \sum_{m,n} (\delta_{m,n} E_m + (1 - \delta_{m,n}) J_{mn}) |m\rangle\langle n| \tag{9}$$

or if it has been diagonalized in the representation of excitonic states

$$H_{\mathrm{ex}} = \sum_{\alpha} \hbar\Omega_\alpha |\alpha\rangle\langle\alpha|. \tag{10}$$

In the first version of H_{ex} the E_m give the electronic excitation energies (site energies) of the various chromophores whereas the J_{mn} are responsible for inter-site Coulomb interaction (usually of the dipole

dipole coupling type). The state $|m\rangle$ describes the presence of a single excitation at chromophore m.

Structural disorder may strongly alternate the J_{mn} whereas energetic disorder reflects itself via fluctuations of the E_m. Both types of static disorder may result in disorder with respect to the excitonic *eigenenergies* E_α and the respective states $|\alpha\rangle$. A (time-dependent) modulation of the E_m and J_{mn} by different types of vibrational modes results in the exciton–vibrational coupling. If one carries out a power expansion with respect to deviations from the ground-state equilibrium position and uses the *eigenstates* representation the coupling reads in the lowest order

$$H_{\text{ex–vib}} = \sum_{\alpha,\beta} \sum_{\xi} \hbar\omega_\xi g_\xi(\alpha,\beta) Q_\xi |\alpha\rangle\langle\beta|. \tag{11}$$

Concentrating on an expansion of the E_m only one obtains

$$g_\xi(\alpha,\beta) = \sum_m C^*_\alpha(m) g_\xi(m) C_\beta(m), \tag{12}$$

where the C_α are the expansion coefficients of the localized states $|m\rangle$ in the exciton state $|\alpha\rangle$, and $-2g_\xi(m)$ gives the dimensionless displacement of the vibrational equilibrium position if site M is in the excited state (for more details see [20]). The Q_ξ in Eq. (11) denote the respective vibrational coordinates (understood here as dimensionless quantities). If a normal-mode analysis is possible the Q_ξ as well as the ω_ξ correspond to normal-mode coordinates and frequencies, respectively. (Otherwise, the latter have only the meaning of a reference energy.) In this case the related vibrational Hamiltonian reads (with respective kinetic energy operator T_{vib})

$$H_{\text{vib}} = T_{\text{vib}} + \sum_\xi \frac{\hbar\omega_\xi}{4} Q_\xi^2. \tag{13}$$

It is worth mentioning that $Q_\xi = C_\xi + C_\xi^+$ where the C_ξ and C_ξ^+ describe harmonic oscillator operator. Of course it might be useful to discuss a coupling among them. But this has been done elsewhere in the framework of the multi-mode Brownian oscillator model [1].

It would be of interest to take the diagonal part $g_\xi(\alpha,\alpha)$ of the coupling matrix $g_\xi(\alpha,\beta)$ and introduce vibrational Hamiltonian valid for the various exciton levels. This simply follows from a rearrangement of H_1, Eq. (8)

$$H_1 = \sum_\alpha H_\alpha |\alpha\rangle\langle\alpha| + \sum_{\alpha\neq\beta} \sum_\xi \hbar\omega_\xi g_\xi(\alpha,\beta) Q_\xi |\alpha\rangle\langle\beta|. \tag{14}$$

The vibrational Hamiltonian for exciton level α is given as

$$H_\alpha = T_{\text{vib}} + U_\alpha^{(0)} + \sum_\xi \frac{\hbar\omega_\xi}{4} \left(Q_\xi + 2g_\xi(\alpha,\alpha)\right)^2. \tag{15}$$

The second and the third terms on the right-hand side form an excitonic PES $U_\alpha(Q)$ with equilibrium value

$$U_\alpha^{(0)} \equiv \hbar\varepsilon_\alpha = \hbar\Omega_\alpha - \sum_\xi \hbar\omega_\xi g_\xi^2(\alpha,\alpha). \tag{16}$$

For further use we write $H_\alpha = \hbar\varepsilon_\alpha + \Delta H_\alpha$, where ΔH_α is the (harmonic oscillator) Hamiltonian of the various vibrational modes displaced by $-2g_\xi(\alpha,\alpha)$. If the inequality $g_\xi(\alpha,\alpha) \gg |g_\xi(\alpha,\beta)|$, $(\alpha \neq \beta)$ is fulfilled this introduction of excitonic PES allows to exactly account for the diagonal coupling matrix and to carry out an perturbation theory with respect to the off-diagonal parts. In Section 5 numbers are given for the diagonal and off-diagonal parts of the exciton vibrational coupling matrix.

3. Reduced density operator formulation of the linear absorption coefficient

As already claimed in the introduction an expression for the absorption coefficient will be of central interest for us which is based on a particular solution of the QME for the exciton density matrix. To characterize the quality of this approximation we refer to some alternative expressions given in Appendices A and B. Although it is possible to start from the site-representation of the CC Hamiltonian (see, e.g. [13,20]) we will exclusively concentrate on those treatments which are based on the use of the electronic *eigenstates*.

We start the discussion with a formula for the absorption (or for $I(\omega)$) which is based on a complete expansion with respect to the exciton

vibrational coupling $g_\xi(\alpha,\beta)$. This formula can be found in Appendix A. It describes the standard expansion of the absorption with respect to vibrational satellites. Therefore, its application is only advisable if one can concentrate on low-order contributions with respect to the exciton vibrational coupling. Any partial summation related to that coupling cannot be carried out. In Appendix B use is made of the excitonic PES introduced in Eq. (15). Now, a partial summation with respect to the diagonal matrix elements $g_\xi(\alpha,\alpha)$ becomes possible, and the perturbation expansion with respect to the off-diagonal coupling matrix elements becomes possible. The lowest-order contribution is given in Appendix B too.

These direct perturbational expansions will be confronted in Sections 3.1 and 3.2 with an approach which uses a certain solution of the QME for the exciton density matrix. A separate consideration of high-frequency vibrational DOF is carried out in Section 3.2 too. To achieve a density matrix formulation, Eq. (2) for the dipole–dipole correlation function needs to be modified. The given form represents an often used starting point for calculations based on many-body techniques. Typically, in this manner one describes the interacting many-electron system of a semiconductor. If molecular systems in a condensed-phase situation are of interest methods of dissipative quantum dynamics are usually the method of the choice. They do not focus on many body effects but account for the coupling of an active system to a certain environment (reservoir). Since we will base our consideration on the QME governing the exciton density matrix a respective formulation of the absorption has to be given. Accordingly a reduced density operator

$$\hat{\rho}(t) = \mathrm{tr}_{\mathrm{vib}}\{\hat{W}(t)\} \tag{17}$$

is introduced which is valid for the active system formed by the electronic ground-state and all single-excited electronic states (exciton states). These electronic DOF form the so-called active system whereas the reservoir is given by the vibrational DOF of the CC. (At a later step of our considerations some selected high-frequency vibrational DOF will be incorporated into the definition of $\hat{\rho}$, too.) According to the formulation of the active (relevant) system $\hat{\rho}(t)$ follows from the total statistical operator $\hat{W}(t)$ as a trace with respect to the vibrational DOF. Furthermore, the correlation function, Eq. (2) is obtained as [22]

$$C_{\mathrm{d-d}}(t) = \mathrm{tr}_{\mathrm{S}}\{\hat{\mu}\hat{\sigma}(t)\}, \tag{18}$$

where the newly introduced density operator takes the form

$$\hat{\sigma}(t) = \mathscr{U}(t)[\hat{\mu},\hat{\rho}_{\mathrm{eq}}]_-. \tag{19}$$

The definition of the time-evolution superoperator $\mathscr{U}(t)$ has to correspond to the choice of the QME (for details see Appendix C). Furthermore, the equilibrium value of the reduced density operator $\hat{\rho}_{\mathrm{eq}}$ is given by the projector $|0\rangle\langle 0|$ on the CC electronic ground-state. (If high-frequency modes are incorporated into the definition of $\hat{\rho}$ the part $|0\rangle\langle 0|$ has to be extended by the vibrational equilibrium statistical operator $\hat{R}_{\mathrm{eq}}$.)

Carrying out an expansion with respect to the electronic *eigenstates*, i.e., the CC ground-state $|0\rangle$ and the states $|\alpha\rangle$ of the first excited CC levels one obtains

$$C_{\mathrm{d-d}}(t) = \sum_\alpha \mathbf{d}_\alpha^* B_\alpha(t) + \mathrm{c.c.} \tag{20}$$

with the transition amplitude from $|0\rangle$ into the states $|\alpha\rangle$

$$B_\alpha(t) = \langle\alpha|\hat{\sigma}(t)|0\rangle. \tag{21}$$

If we introduce the half-sided Fourier-transform $\tilde{B}_\alpha(\omega)$ of the transition amplitude we obtain

$$I(\omega) = \mathrm{Re}\sum_\alpha (\mathbf{d}_\alpha^*\tilde{B}_\alpha(\omega) + \mathbf{d}_\alpha\tilde{B}_\alpha^*(-\omega)). \tag{22}$$

3.1. Inclusion of non-Markovian contributions

As already mentioned the density matrix description of the absorption will be of central interest for our studies and will be used to give an alternative to Eqs. (A.3) and (B.1). It is based on Eq. (18) with a density operator obtained according to Eq. (19). For its propagation we assumed that the vibrational DOF should form a thermal reservoir entering the respective density matrix equation via energy relaxation and dephasing rates. In the case of linear absorption one has to calculate electronic off-diagonal matrix

elements of the density operator as introduced in Eq. (21). The respective equation of motion has been derived in Appendix C, Eq. (C.17) and reads

$$\frac{\partial}{\partial t}B_\alpha(t) = -\mathrm{i}\Omega_\alpha B_\alpha(t) - \sum_{\beta,\gamma}\int_0^{t-t_0} \mathrm{d}\tau \mathrm{e}^{-\mathrm{i}\Omega_\beta\tau} C_{\alpha\beta\beta\gamma}(\tau) \times B_\gamma(t-\tau). \tag{23}$$

First we shortly indicate how the time-dependent approach recovers an absorption spectrum with homogeneous broadened exciton levels. To this end the dissipative part governed by the correlation function, Eq. (C.6) has to be reduced to a simple dephasing rate Γ_α, Eq. (C.19). Details of this approximation have been given in Appendix C. Accordingly, the right-hand side of Eq. (23) reduces to $-\mathrm{i}(\Omega_\alpha - \mathrm{i}\Gamma_\alpha)B_\alpha$, and the respective equation of motion can be simply solved leading to the following analytical expression of I (positive frequency part only):

$$I(\omega) = \sum_\alpha |\mathbf{d}_\alpha|^2 \frac{\Gamma_\alpha}{(\omega-\Omega_\alpha)^2+\Gamma_\alpha^2}. \tag{24}$$

This formula is a generalization of the expression (5), with homogeneous line-broadening given via the dephasing rates Γ_α. However, there is no deviation from a simple Lorentzian line-shape, and not any mixture of different exciton levels appears.

Next it is demonstrated how an improvement of the Lorentzian line shape of the absorption, Eq. (24) can be achieved by including non-Markovian contributions to the QME. Although the whole approach can be formulated via standard Green's functions defined in the frequency domain [20] here we demonstrate how the result can be obtained from the non-Markovian QME. According to Eqs. (19) and (18) we have to note that the propagation of $\hat{\sigma}$ (or more specifically of $B_\alpha(t)$) starts at $t_0 = 0$. Following Eq. (22) where $I(\omega)$ has been given by the half-sided Fourier-transform $\tilde{B}_\alpha(\omega)$ of $B_\alpha(t)$, it becomes necessary to transform the non-Markovian QME, (23) into the following equation for $\tilde{B}_\alpha(\omega)$:

$$-\mathrm{i}(\omega-\Omega_\alpha)\tilde{B}_\alpha(\omega) = \mathbf{d}_\alpha - \sum_{\beta,\gamma}\tilde{C}_{\alpha\beta,\beta\gamma}(\omega-\Omega_\beta)\tilde{B}_\gamma(\omega). \tag{25}$$

The half-sided Fourier-transform $\tilde{C}$ of the correlation function is given in Eq. (C.8).

An analytical formula which generalizes Eq. (24) is obtained if we neglect all parts of $\tilde{C}_{\alpha\beta,\beta\gamma}$ where γ is different from α. In this case it follows (note the neglect of the non-resonant contributions):

$$I(\omega) = \sum_\alpha |\mathbf{d}_\alpha|^2 \frac{\Gamma_\alpha(\omega)}{(\omega-\Omega_\alpha-\Sigma_\alpha(\omega))^2+\Gamma_\alpha^2(\omega)} \tag{26}$$

with

$$\begin{aligned}\Sigma_\alpha(\omega) - \mathrm{i}\Gamma_\alpha(\omega) &= -\mathrm{i}\sum_\beta \tilde{C}_{\alpha\beta,\beta\alpha}(\omega-\Omega_\beta) \\ &= \sum_\beta\sum_\xi \omega_\xi^2 |g_\xi(\alpha,\beta)|^2 \\ &\quad\times\left(\frac{1+n(\omega_\xi)}{\omega-\Omega_\beta-\omega_\xi+\mathrm{i}\varepsilon}+\frac{n(\omega_\xi)}{\omega-\Omega_\beta+\omega_\xi+\mathrm{i}\varepsilon}\right).\end{aligned} \tag{27}$$

Expression (26) generalizes formula (24) for the absorption coefficient in two ways. First, the line-broadening became frequency dependent. And second, the resonance frequencies Ω_α have been shifted by the (frequency–dependent) quantity $\Sigma_\alpha(\omega)$. We note that the Markovian result Eq. (24) does not include a line shift because the imaginary part of the exciton–vibrational correlation function has been neglected. Otherwise a frequency independent line shift Σ_α results and would appear in the denominator of Eq. (24). Furthermore, Eq. (26) for the absorption indicates that a partial summation with respect to the complete exciton–vibrational coupling has been achieved. Of course, the result is different from the complete summation contained in Eq. (A.3). An improvement of Eq. (26) is possible by a numerical solution of Eq. (25).

For further comparison we will use Eq. (25) to compute the first vibrational satellite. Therefore, $\tilde{B}_\alpha(\omega)$ is approximated up to the second order in the exciton–vibrational coupling (note $\tilde{\omega} = \omega + \mathrm{i}\varepsilon$)

$$\tilde{B}_\alpha(\omega) \approx \frac{\mathrm{i}\mathbf{d}_\alpha}{\tilde{\omega}-\Omega_\alpha} - \sum_{\beta,\gamma}\frac{\tilde{C}_{\alpha\beta,\beta\gamma}(\omega-\Omega_\beta)\mathbf{d}_\gamma}{(\tilde{\omega}-\Omega_\alpha)(\tilde{\omega}-\Omega_\gamma)}. \tag{28}$$

A generalization of this expression will be derived in the following section. Here we only note that the

first term would result in the main exciton absorption whereas the vibrational satellite (related to a single vibrational quantum) is given by the second term.

3.2. Inclusion of high-frequency vibrations

Next we present an approach which allows to handle high-frequency vibrations separately if it gives rise to clearly identifiable vibrational satellites. A broadening of the exciton levels will be accounted for by the coupling to low-frequency vibrational modes. Therefore, high-frequency (hf) vibrational modes together with the exciton levels define the active system and the reservoir is given by the low-frequency vibrations. (Note that the given description of the vibrational DOF does not correspond to the widely used multi-mode Brownian oscillator model [1].) Consequently, the active-system Hamiltonian has to be identified with the high-frequency mode vibrational Hamiltonian $H_{\rm hf}$ for the CC electronic ground-state and with H_1, Eq. (8). In the latter expression again the vibrational DOF have to be restricted to the high-frequency modes. Furthermore, Eq. (17) defining the reduced density operator has to be specified to $\hat{\rho}(t) = {\rm tr}_{\rm lf}\{\hat{W}(t)\}$, where the trace corresponds to the low-frequency (reservoir) modes. The transition amplitude reads as

$$B_\alpha(t) = \langle\alpha|{\rm tr}_{\rm hf}\{\hat{\sigma}(t)\}|0\rangle. \tag{29}$$

In the following we will construct a perturbation expansion with respect to the coupling $H_{\rm ex\text{–}hf}$ between the excitons and the high-frequency vibrations. This can be achieved by the perturbational treatment of the equation of motion for the transition amplitude, Eq. (29). Such an equation is simply obtained from the density matrix Eq. (C.15) in noting the generalization of the transition amplitude

$$\begin{aligned}\frac{\partial}{\partial t}B_\alpha(t) &= -\frac{\rm i}{\hbar}\langle\alpha|{\rm tr}_{\rm hf}\{(H_{\rm ex}+H_{\rm ex-hf})\hat{\sigma}(t)+[H_{\rm hf},\hat{\sigma}(t)]_-\}|0\rangle \\ &\quad -\Gamma_\alpha B_\alpha(t).\end{aligned} \tag{30}$$

The commutator with respect to $H_{\rm hf}$ vanishes since it appears under the trace. Note that Γ_α is the result of the exclusive coupling to the low-frequency vibrational DOF. As a convenient abbreviation we define complex exciton frequencies

$$\tilde{\Omega}_\alpha = \Omega_\alpha - {\rm i}\Gamma_\alpha. \tag{31}$$

The appearance of $H_{\rm ex\text{–}hf}$ in Eq. (30) leads to the (single) vibrational quantum assisted transition amplitude $L^{(\pm)}(\xi,\alpha;t) = \langle\alpha|{\rm tr}_{\rm hf}\{C^\pm_\xi\hat{\sigma}(t)\}|0\rangle$. To have a short-hand notation $C^\pm_\xi$ has been introduced referring to C^+_ξ and $C^-_\xi \equiv C_\xi$, respectively. Accordingly, Eq. (30) results in

$$\begin{aligned}\frac{\partial}{\partial t}B_\alpha(t) &= {\rm i}\tilde{\Omega}_\alpha B_\alpha(t) - {\rm i}\sum_{\beta,\xi}\omega_\xi g_\xi(\alpha\beta)(L^{(-)}(\xi,\beta;t) \\ &\quad + L^{(+)}(\xi,\beta;t)).\end{aligned} \tag{32}$$

The complete hierarchy of equations of motion for all types of multi-vibrational quantum assisted transition amplitudes gives all vibrational satellites. Since single-quantum assisted contributions to the absorption are of main interest the equation of motion for $L^{(\pm)}(\xi,\beta;t)$ is decoupled from the hierarchy of higher functions. We note

$$\begin{aligned}&\frac{\partial}{\partial t}L^{(\pm)}(\xi,\beta;t) \\ &\quad = -{\rm i}(\tilde{\Omega}_\beta \mp \omega_\xi)L^{(\pm)}(\xi,\beta;t) - {\rm i}\sum_{\gamma,\bar{\xi}}\omega_{\bar{\xi}}g_{\bar{\xi}}(\beta\gamma) \\ &\qquad \times\langle\gamma|{\rm tr}_{\rm hf}\{C^\pm_\xi Q_{\bar{\xi}}\hat{\sigma}(t)\}|0\rangle\end{aligned} \tag{33}$$

and replace $C^\pm_\xi Q_{\bar{\xi}}$ by its thermal expectation value to get $\delta_{\xi,\bar{\xi}}n(\omega_\xi)$ and $\delta_{\xi,\bar{\xi}}(1+n(\omega_\xi))$, respectively. Integrating the resulting equation and inserting the result into Eq. (32) gives a closed equation for the transition amplitude which is identical with Eq. (23) except two points. First, the correlation function is exclusively defined by the high-frequency vibrational DOF (we will write $C^{(\rm hf)}$). And second, any frequency Ω_α has to be replaced by the complex quantity, Eq. (31) [23].

In similarity to Eq. (22) we can determine the absorption by the half-sided Fourier-transform $\tilde{B}_\alpha(\omega)$ of $B_\alpha(t)$. Restricting to a formula which only incorporates contributions up to the first high-frequency vibrational satellite the related approximate solution for $\tilde{B}_\alpha(\omega)$ reads (note the possible replacement of $\tilde{\omega}$ by the real quantity ω)

$$\tilde{\boldsymbol{B}}_{\alpha}(\omega) \approx \frac{\mathrm{i}\mathbf{d}_{\alpha}}{\omega - \tilde{\Omega}_{\alpha}} + \sum_{\beta,\gamma} \frac{\tilde{C}^{(\mathrm{hf})}_{\alpha\beta,\beta\gamma}(\omega - \tilde{\Omega}_{\beta})\mathbf{d}_{\gamma}}{(\omega - \tilde{\Omega}_{\alpha})(\omega - \tilde{\Omega}_{\gamma})}. \tag{34}$$

This expression is similar to that given in Eq. (28) but restricted here on vibrational satellites originating from the high-frequency modes together with a broadening of the exciton levels caused by the low-frequency vibrational DOF. ($\tilde{C}^{(\mathrm{hf})}_{\alpha\beta,\beta\gamma}$ is simply obtained as the generalization of the quantity in Eq. (27) to the set of quantum numbers $(\alpha\beta,\beta\gamma)$ but in using the high-frequency vibrational mode correlation function.) We insert Eq. (34) into Eq. (18) and get the absorption cross section as

$$I(\omega) = \sum_{\alpha} \frac{|\mathbf{d}_{\alpha}|^2 \Gamma_{\alpha}}{(\omega - \Omega_{\alpha})^2 + \Gamma_{\alpha}^2} - \mathrm{Re} \sum_{\alpha,\beta,\gamma} \frac{\mathbf{d}^{*}_{\alpha}\tilde{C}^{(\mathrm{hf})}_{\alpha\beta,\beta\gamma}(\omega - \tilde{\Omega}_{\beta})\mathbf{d}_{\gamma}}{(\omega - \tilde{\Omega}_{\alpha})(\omega - \tilde{\Omega}_{\gamma})}. \tag{35}$$

To compute higher-order contributions within this frame becomes a difficult task. However, if the inequality $g_{\xi}(\alpha\alpha) \rangle |g_{\xi}(\alpha\beta)|, \alpha \neq \beta$ is valid it might be possible to concentrate on those contributions which are exclusively caused by the diagonal coupling matrix elements. In this manner vibrational progression beyond the single-quantum assisted transition can be accounted for. To do this we follow Appendix B and split off the active system Hamiltonian $H_{\mathrm{ex}} + H_{\mathrm{ex\text{–}hf}} + H_{\mathrm{hf}}$ according to Eq. (14). But now the vibrational Hamiltonian H_{α} describes the high-frequency mode dynamics in the excitonic PES. If this new separation of the Hamiltonian has been introduced into the equation of motion (30) an integration becomes possible after neglecting the off-diagonal contribution of the exciton (high-frequency) vibrational coupling. It yields

$$C_{\mathrm{d\text{–}d}}(t) = \sum_{\alpha} |\mathbf{d}_{\alpha}|^2 \mathrm{e}^{-\Gamma_{\alpha} t} \mathrm{tr}_{\mathrm{hf}}\{\hat{R}_{\mathrm{hf}} U^{+}_{\mathrm{hf}}(t) U_{\alpha}(t)\}. \tag{36}$$

The trace is similar to that in Eq. (B.5) but restricted here to the high-frequency vibrational DOF. According to Eq. (B.6) the above given expression for the dipole–dipole correlation function can be expressed via the line-shape function, Eq. (B.7).

For further use let us shortly indicate the derivation of the absorption if only a single high-frequency mode is present. In this case the spectral density equation (C.7) simply reads

$$J_{\alpha\alpha,\alpha\alpha}(\omega) = g^2(\alpha\alpha)\delta(\omega - \omega_{\mathrm{hf}}). \tag{37}$$

Assuming $k_{\mathrm{B}}T \ll \hbar\omega_{\mathrm{hf}}$ the lineshape function, Eq. (B.7) follows as:

$$s_{\alpha}(t) = g^2(\alpha\alpha)\mathrm{e}^{-\mathrm{i}\omega_{\mathrm{hf}} t}. \tag{38}$$

Finally the absorption is obtained as

$$\alpha(\omega) = \frac{4\pi\omega n_{\mathrm{CC}}}{\hbar c} \sum_{\alpha} |\mathbf{d}_{\alpha}| \mathrm{e}^{-g^2(\alpha\alpha)} \times \sum_{n=0}^{\infty} \frac{g^{2n}(\alpha\alpha)}{n!} \frac{\Gamma_{\alpha}}{(\omega - \varepsilon_{\alpha} - \omega_{\mathrm{hf}})^2 + \Gamma_{\alpha}^2}, \tag{39}$$

which is not completely standard since shifted and broadened excitonic energies $\hbar\varepsilon_{\alpha}$ are included.

4. Linear absorption of dendrimers

Since a couple of years dendrimeric molecular systems received much interest, on the one-hand side because of their self-similar structure and on the other-hand side because of their potential applicability in different fields of chemistry [21,24–27] (for a recent overview on the literature see also [28]). Here, we will concentrate on the particular type of dendrimers: the compact phenylacetylene dendrimers. Different so-called generation of this molecule are created by the repetition of the basic structure D1 (or D5, compare Figs. 1 and 2) of four phenyl rings and three acetylene groups. Every generation is labeled by the number of repetitions (D2, D3, D4, etc.) or by the number of phenyl rings D4 instead of D1 followed by D10, D22, D46, and D94. The specification *compact* dendrimers refers to the fact that the various phenyl rings are only connected by single acetylene groups (see Fig. 2). In the couple of theoretical papers [28–32] these phenylacetylene dendrimers have been considered, and, in particular, the validity of a Frenkel-exciton model, Eq. (9) to describe the electronic excitations has been justified as well as its applicability to understand optical and transport properties.

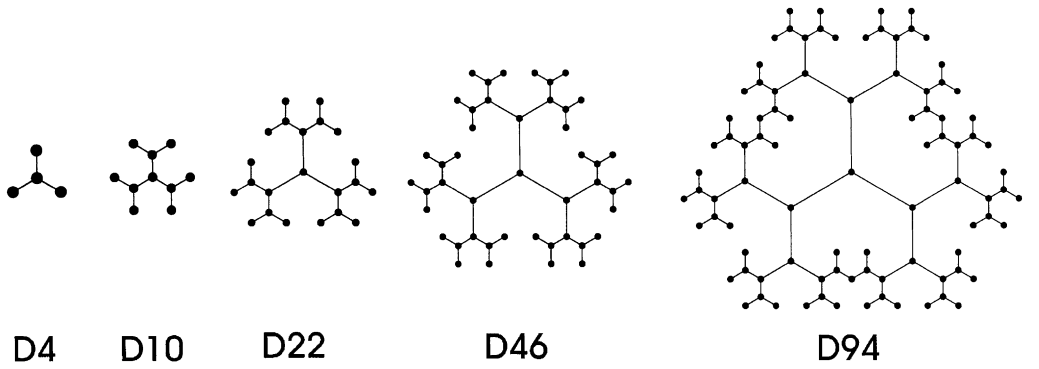

Fig. 1. Structure of different generations (D4–D94) of compact phenylacetylene dendrimers. Points stand for phenyl rings, lines for acetylene groups. All branches are of the same length, for the two-dimensional presentation the acetylene groups of the center are extended.

It is far from being an obvious conclusion that the Frenkel-exciton model can be applied to the molecular structure of phenylacetylene dendrimers. But the quantum chemical calculations of [29] gave clear hints for its usage. Accordingly, the phenyl group between two acetylene rings can be interpreted as the site characterized by the local excitation energy E_m. All these sites are coupled by nearest-neighbor inter-site coupling energies J_{mn} resulting in a Hamiltonian like that of Eq. (9). Although a detailed characterization of the electronic properties including two-exciton states can be found in [29–31] a consideration of the coupling to vibrational degrees of freedom has only been given recently in [28]. Here, we will concentrate on this aspect together with the influence of structural and energetic disorder.

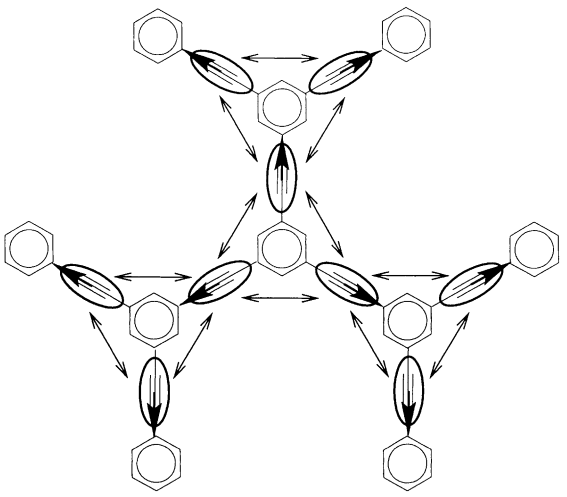

Fig. 2. Schematic picture of the chromophores of D10 and their interaction in the Frenkel-exciton model. The ellipses mark the chromophores at the acetylene threefold bonds. The transition dipole moments are aligned with the bondings, marked with the big arrows. Only next-neighbor interaction is taken into account (double arrows).

4.1. Long-wavelength tail of the absorption

First our computations will be devoted to a detailed study of the long-wavelength tail of the absorption spectra at the 320 nm position of the 0–0 transition as measured in [21] for the different generations (D4–D94). Since the 0–1 transition is separated from the 0–0 transition more than 10 nm, and does not substantially change its shape with increasing generation number, and the long wavelength tail extends up to 30 nm above the 0–0 transition such an approach seems to be justified. (Vibrationally assisted transitions will be discussed in a second step and are explained in Section 4.2.)

Fig. 3 displays the position of the fundamental absorption lines (exciton energies $\hbar\Omega_\alpha$) of compact dendrimers. Additionally the oscillator strength $\sim |\mathbf{d}_\alpha|^2$ is given showing a concentration in the 320 nm region. The influence of homogeneous broadening according to a formula like Eq. (24) has been already described in [30]. Here the basic hypothesis will be the assumption that static disorder substantially determines the spectra; and it will be

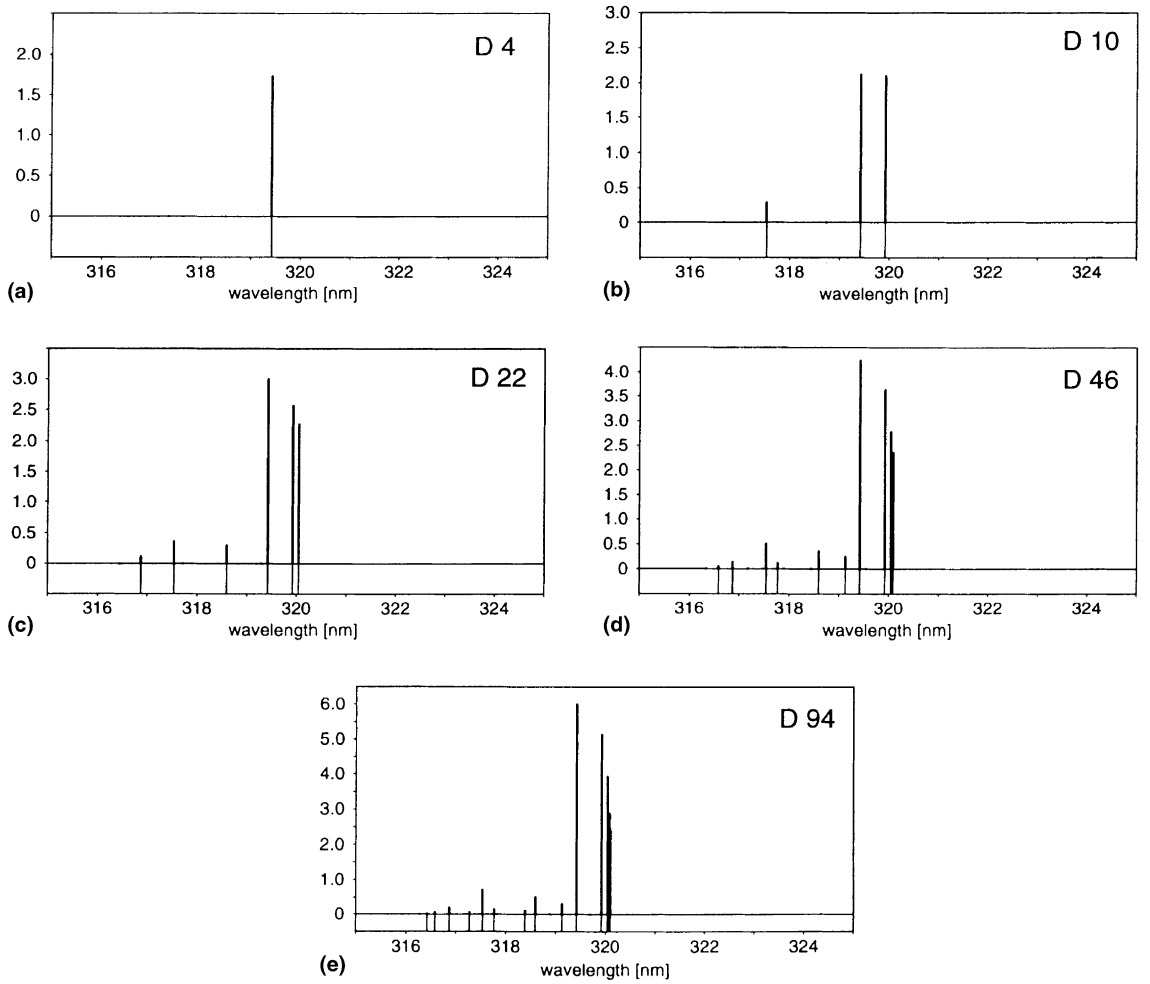

Fig. 3. Energetic position of the fundamental absorption lines for compact phenylacetylene dendrimer generations D4–D94 (a)–(e). The length of the vertical lines corresponds to the oscillator strength for the idealized case of the absence of static as well as dynamic disorder. (For a clear identification of those lines with a small oscillator strength the positions of all lines are marked in the lower part of the figures.) For the nearest-neighbor coupling constants we used -68 cm^{-1} [30].

tested whether or not there is a change of (structural and energetic) disorder from the center to the peripherical part of the dendrimer. Such an investigation seems to be useful since the coupling of the outer part of the macromolecule to the solvent molecules should be stronger and should introduce various deviations from the ideal structure.

To this end a standard Monte Carlo approach will be used where energetic and structural disorder is accounted for by randomly chosen site-energies E_m and inter-site couplings J_{mn} belonging to the Frenkel-exciton Hamiltonian Eq. (9) (compare, e.g. [9,18,13]). The change of the disorder influence onto different parts of the molecule is modeled via increasing fluctuations of the various E_m and J_{mn} from the inner to the outer part of the dendrimer. A direct access to such a site-specific disorder would be obtained via MD simulation of dissolved dendrimers. Here, we will follow an easier way and will compare different types of an *ansatz* for this variation. Therefore we introduce Δr as the distance between the centers of neighboring acetylene

groups in the dendrimer (distance between neighboring sites). Then, the width of the particular energy fluctuation should vary from generation to generation with $x = \mathcal{N}\Delta r/r_{\text{char}}$, where $\mathcal{N}$ counts the generation and r_{char} represents a characteristic reference length. We have used the functions $x, x^2, 2^x, 5^x$, and 10^x. The results for the exclusive presence of diagonal and off-diagonal disorder in the D22 dendrimer are shown in Figs. 5 and 6, respectively. All spectra have been obtained by generating 1000 configuration and, afterwards, by smoothing out the resulting configuration averaged absorption. For comparison the homogeneous broadening of the D22 absorption is given in Fig. 4.

A detailed inspection of all absorption curves shows a strong dependence on the used disorder model. In particular off-diagonal disorder results in a very structured line shape. Comparing the different shapes with the one measured in [21] (see Fig. 7) one may conclude that diagonal disorder with an increase of the site energy fluctuations according to $5^{(\mathcal{N}\Delta r/r_{\text{char}})}$ seems most appropriate if related to the other introduced models.

4.2. Vibrational satellites

Vibrational satellites of the main excitonic transitions are visible in the experimental absorption spectra of all generations of compact dendrimers (see [21]). In a first attempt we used Eq. (35) to compute the measured absorption. However, better agreement could be achieved when simu-

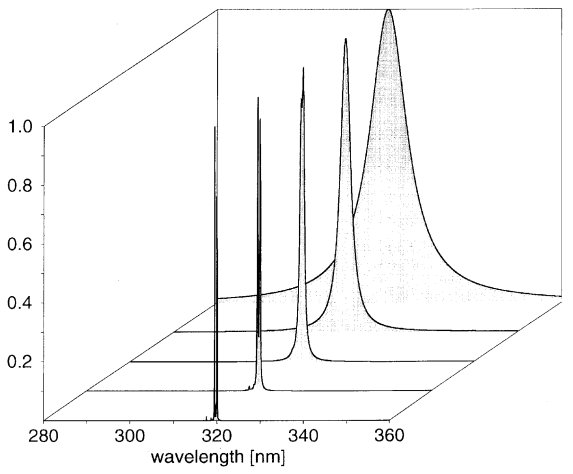

Fig. 4. Absorption lineshape corresponding to the phenylacetylene dendrimer generation D22 with the exclusive incorporation of homogeneous line-broadening $\Gamma_\alpha = 2, 8, 32, 128$, and 512 cm^{-1} (from the front panel to the background).

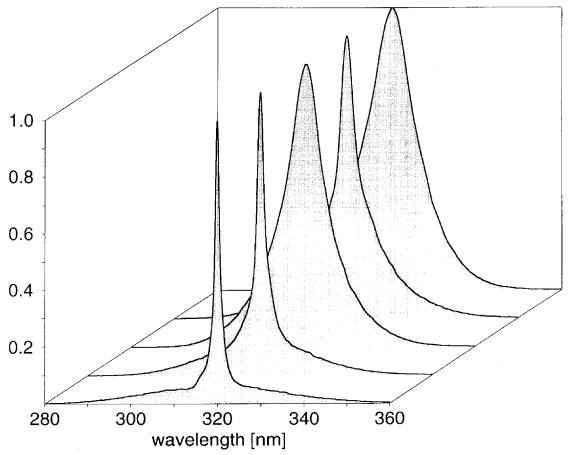

Fig. 5. Absorption lineshape corresponding to the phenylacetylene dendrimer generation D22 with the exclusive incorporation of energetic disorder (diagonal disorder with respect to the site-representation). The disorder increases from the center to the periphery with different functional dependences: linear (x), quadratic $(x^2), 2^x, 5^x$, and 10^x (from the background to the front panel).

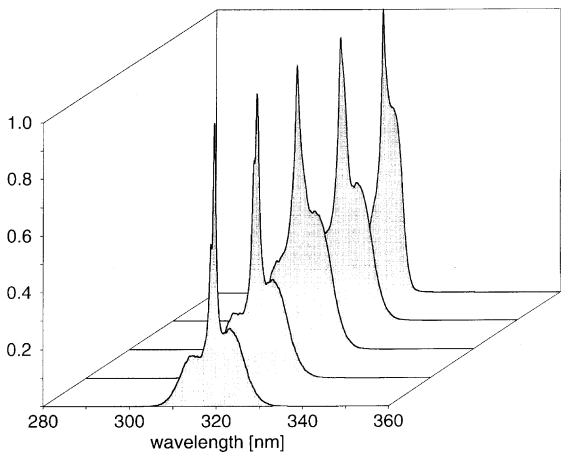

Fig. 6. Absorption lineshape corresponding to the phenylacetylene dendrimer generation D22 with the exclusive incorporation of structural disorder (off-diagonal disorder with respect to the site-representation) The disorder increases from the center to the periphery with different functional dependences: linear (x), quadratic $(x^2), 2^x, 5^x$, and 10^x (from the background to the front panel).

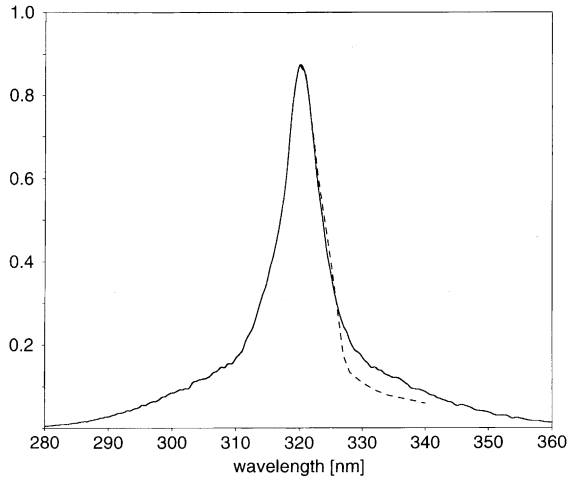

Fig. 7. Simulation of the absorption spectrum of D22 (solid line) in comparison with the long wavelength tail of the experimental absorption spectra [21] (dashed line). The diagonal disorder goes with x^5.

lating the absorption spectra according to Eq. (39), but introducing two different vibrational modes. For simplicity, static disorder has been neglected. The vibration with the higher frequency $\omega_{\mathrm{hf}}^{(1)}$ has the fixed energy of $\hbar\omega_{\mathrm{hf}}^{(1)} = 1936\ \mathrm{cm}^{-1}$ in all generations of the dendrimer. In contrast the vibration with the lower frequency $\omega_{\mathrm{hf}}^{(2)}$ shifts from $\hbar\omega_{hf}^{(2)} = 1008\ \mathrm{cm}^{-1}$ in generations 1–3 to $\hbar\omega_{hf}^{(2)} = 1065\ \mathrm{cm}^{-1}$ in generation 4 and $\hbar\omega_{hf}^{(2)} = 1170\ \mathrm{cm}^{-1}$ in generation 5. (Note that spectra shown in Fig. 8 have been obtained in neglecting combination frequencies.)

Since the experimental spectra get broader due to higher disorder in higher generations, in this simple model a dephasing rate of $\Gamma_\alpha = 645\ \mathrm{cm}^{-1}$ for the first generations, $\Gamma_\alpha = 726\ \mathrm{cm}^{-1}$ for the fourth and $\Gamma_\alpha = 968\ \mathrm{cm}^{-1}$ for the fifth generation has been introduced. Due to this high spectral broadening and the much lower coupling between the chromophores one cannot distinguish the different excitonic contributions to the absorption spectrum. The displacement parameter $g^2(\alpha,\alpha)$ is determined to be 0.5 for the vibration with the larger frequency and 0.39 for that with the lower frequency. With these parameters we can fairly well reproduce the vibrational features of the experimental spectra of [21].

5. Linear absorption of chlorophyll–protein complexes

At the present time the microscopically best characterized class of chromophore complexes (on an Å length scale) is given by a selected number of

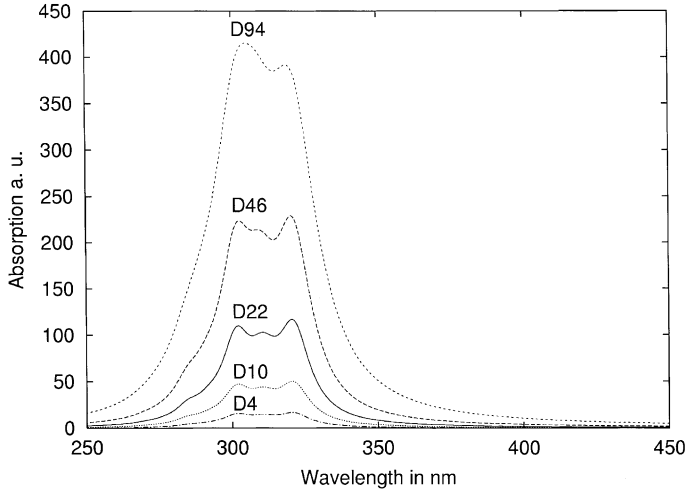

Fig. 8. Simulation of the short wavelength part of the absorption spectrum of D4–D94 including vibrational satellites. Parameters are discussed in Section 4.2.

CC of photosynthetic active biological systems. CC which contains as photoactive pigments different variants of chlorophyll molecules (Chl) and carotenoids fulfill a light harvesting function. The light energy that is absorbed in these so-called antenna systems is transferred to the photosynthetic reaction center where it drives charge transfer reactions. The pigments of the photosynthetic antennae are held in position by a scaffold of membrane-bound proteins. Energy transfer between the pigments occurs via an exciton mechanism [33].

The pigment–protein interaction plays a crucial role for the functionality of the antennae. Different binding sites in the protein lead to different microscopic environments of the pigments. The optical transition energies of the pigments experience a modulation by the protein dynamics. The slow conformational motion of the protein with large amplitude can be considered as static disorder which leads to an inhomogeneous broadening of the absorption spectrum of the antenna. The homogeneous broadening of the optical transitions is determined by the fast and small-amplitude motion of the protein on a pico- and femtosecond time scale. The static disorder together with the heterogeneity in binding sites helps to increase the absorption cross section of the antenna system to achieve absorption of sun light in a broad spectral range. The reaction center absorbs at the energetic bottom of the antenna absorption spectrum. Hence, the spatial transfer of excitation energy is related with a spectral relaxation. The electronic excess energy is dissipated into the protein. The latter process is triggered by the fast protein dynamics, the dynamic disorder.

It is a challenge for the theory to understand the complex scenario of the absorption process in photosynthetic antennae. Starting from structural information the inter-pigment couplings can be estimated. However, little is known about how the different binding sites in the protein shift the electronic transition energies of the pigments. Therefore, these energies have to be considered as parameters. The local dynamic disorder will be described by the spectral density $J(\omega)$, Eq. (C.13). There is no direct way to obtain this quantity. However, from vibrational side bands seen in high resolution optical spectra on CC the shape and amplitude (the so-called Huang–Rhys factor) of $J(\omega)$ can be estimated.

To describe linear optical absorption we can use the CC Hamiltonian, Eq. (6). The use of the exciton eigenstates $|\alpha\rangle$ is essential for the following since only in this representation a correct description of exciton relaxation can be achieved. The various protein vibrations described by the coordinates Q_ξ are comprised in $H_{\rm vib}$, Eq. (13) whereas their coupling to the excitonic states is contained in Eq. (11). To obtain a sufficient sophisticated expression for $I(\omega)$ which considers the dipole–dipole coupling and exciton–vibrational interaction we use the results of Section 3.2.

5.1. The temperature dependence of the absorption spectrum

In the following we will apply the approach to simulate the temperature dependent absorption of a CC located in the light harvesting complex LHC-II of higher plants. The importance of exciton effects for the interpretation of absorption spectra of the LHC-II has been recognized earlier [34,35]. A recent review on the energy transfer function of the LHC-II can be found in [36]. Since the interaction between CC monomers (which are arranged as trimers in the LHC-II) is weak, the absorption can be simulated in using a monomer model. From the structural investigations of [37] it is known that the LHC-II monomer contains 12 Chl. According to their arrangements in relation to the carotenoids they were tentatively assigned to 7 Chl*a* and 5 Chl*b* (see Fig. 9).

Recent mutation studies [38,39] confirmed a large part of the original assignment, but revealed also some differences. In [39] it was found that the originally assigned Chl_{b3} is a Chl_a whereas a mixed binding of Chl_a and Chl_b was suggested for this site in [38]. In addition, the latter study also found further mixed sites at the originally assigned sites of Chl_{a3}, Chl_{a6}, and Chl_{a7}. And, it was found in [38] that the originally assigned Chl_{b1} is likely to be a Chl_a.

Besides the assignment of the Chl species another uncertainty concerns the direction of the Q_y transition dipole moments. The resolution of the

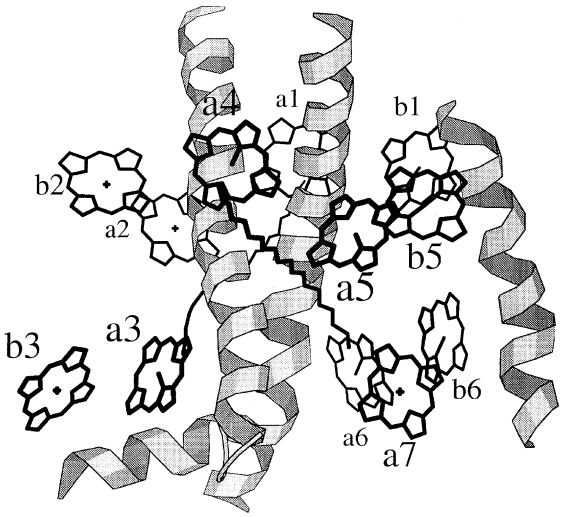

Fig. 9. Schematic cross-section view on the LHC-II monomer according to Kühlbrandt et al. [37]. The mutual position of the 5 Chl*a* and 7 Chl*b* (shown by their tetrapyrrole ring only) is drawn together with the three α-helices spanning the membrane. Graphics prepared using MOLSCRIPT (P.J. Kraulis, J. Appl. Crystall. 24 (1991) 946).

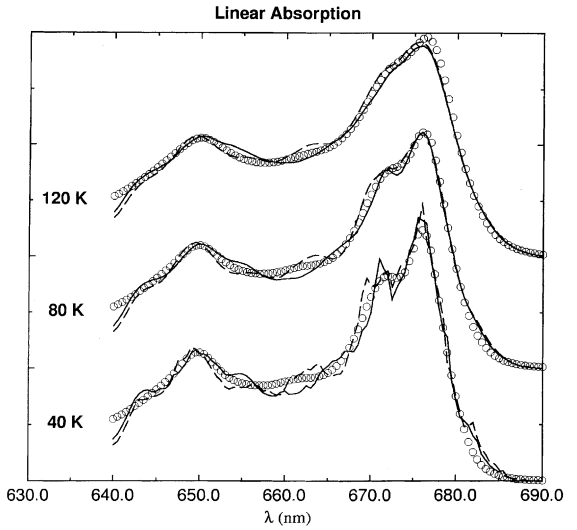

Fig. 10. Linear absorption of the LHC-II for three different temperatures within two structural models. Dashed line: Kühlbrandt model. Solid line: modified Kühlbrandt model (Chl$a_6 \leftrightarrow b_5$). Circles give the experimental values of [50]. The sharp features in the 40 K spectra are due to the finite ensemble size (1000) used for the statistical average.

electron diffraction experiment did not give the exact orientation of the Q_y optical transition dipole moments of the 12 Chl. Instead, two orientations are possible for each Chl. In [40,41] extensive exciton simulations of global features of polarized absorption spectra and energy transfer kinetics could be used to reduce the number of possible dipole configurations from 2^{12} to 9 (for original Chl assignment of Kühlbrandt et al. [37]) or 15 (for a modified Kühlbrandt model in which Chla_6 changes its identity with b_5, see Fig. 9).

We used the above two models for a simulation of the temperature dependence of linear absorption [42]. Within both structural models a reasonable fit of the linear absorption spectrum can be obtained as it is shown in Fig. 10 [43]. The fit of the 77 K circular dichroism spectrum which is shown in Fig. 11 could be used to discriminate between the above two structural models. In the light of the aforementioned mutation studies it is, however, possible that also the structural model which our simulation favors does not include the ultimate assignment of pigments. It can be expected that the fit of the CD signal shown in Fig. 11 can be improved further when there will be higher resolution structural data of the LHC-II available.

It is our goal in the following to see what general information can be obtained from our fit of the linear absorption which will not change upon future refinement of the structural model. To keep the number of adjustable parameters as small as possible we assumed the same inhomogeneous width of the distribution function for the site energies. The determined value of 140 cm^{-1} can be expected to be useful for future simulations. The resulting inhomogeneous width of the lowest exciton transition (which is smaller than the above value because of motional narrowing) was calculated as 85 cm^{-1} which is in reasonable agreement with a width of 70 cm^{-1} determined in hole burning experiments [44].

The dynamic disorder of the site energies was characterized by the Huang Rhys factors $S_a = 0.95$ assumed equal for all Chl_a and $S_b = 0.75$ for Chl_b. These values have been obtained also from the fit of the absorption spectra. The shape $j(\omega)$ of the spectral density $J_m(\omega) = S_m j(\omega)$ (m = Chl*a* or

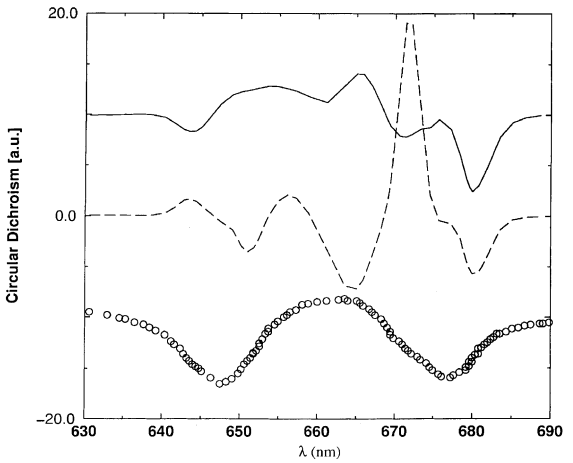

Fig. 11. 77 K circular dichroism spectra within the two models described in Fig. 10 (solid and dashed lines) compared to experimental values of [51] (circles).

Chl*b*) was estimated from the low-temperature fluorescence band [35]. The normalized function $j(\omega)$ is of the type $j(\omega) \sim \omega \exp\{-(\omega/\omega_c)^p\}$, with $p = 0.5$ and $\hbar\omega_c = 6\ \mathrm{cm}^{-1}$, which puts the maximum of the spectral density at $\hbar\omega = 24\ \mathrm{cm}^{-1}$. This local exciton–vibrational coupling leads to a Huang Rhys factor of 0.8 for the lowest exciton state [42] in agreement with hole burning experiments [44].

5.2. Exciton life-times

In the following it shall be investigated which exciton life-times can be predicted from the above obtained homogeneous and inhomogeneous line width of LHC-II exciton transitions. Within the Markov approximation the life time T_α of the exciton state α is obtained from the real part of the exciton–vibrational correlation function, Eq. (C.9)

$$\tau_\alpha = \left(2 \sum_\beta \mathrm{Re}\tilde{C}_{\alpha\beta,\beta\alpha}(\omega_{\alpha\beta}) \right)^{-1}. \tag{40}$$

In the presence of static disorder a probability density $p_\tau(\omega)$ to find at a given frequency (for example in a photon echo experiment) a certain life time may be defined as

$$p_\tau(\omega) = \frac{\left\langle \sum_\alpha \delta(\tau - \tau_\alpha)\delta(\omega - \Omega_\alpha) \right\rangle_{\mathrm{dis}}}{\langle \delta(\omega - \Omega_\alpha) \rangle_{\mathrm{dis}}}. \tag{41}$$

The probability $P_\omega(\tau_1, \tau_2)$ to find at a frequency ω a lifetime τ in an interval $\tau_1 < \tau < \tau_2$ is then easily derived via a respective time-integration. The probabilities of life times for the LHC-II obtained from the parameters determined from the linear absorption spectrum are shown in Fig. 12. The center of the spectrum is determined by sub-picosecond exciton life-times. At high energies there appear life times on a few picosecond. On the red side, in addition, very long life times (larger than 10 ps) are obtained. The latter are caused by the fact that the lowest exciton state can only be depopulated by thermal activation. If the energy gap to the next higher exciton state is large compared to the thermal energy (a temperature of 77 K was assumed) a long life time results for the lowest exciton state. The life times found in the center and in the blue part of the spectrum are in agreement with time resolved pump-probe spectra measured at 77 K by Visser et al. [45]. In this experiment it was found that the exciton relaxation from high to low energies occurs with transfer times of 300 fs (40%), 600 fs (40%) and 4–9 ps (20%). The multi-exponentiality of the transfer can be assumed to arise from heterogeneity and static disorder. For the red part of the spectrum life times of 400 fs (around 672 nm), 2.4 ps (around 661 nm) and a slow component in the 10–20 ps range were found in [45]. These components are also present in

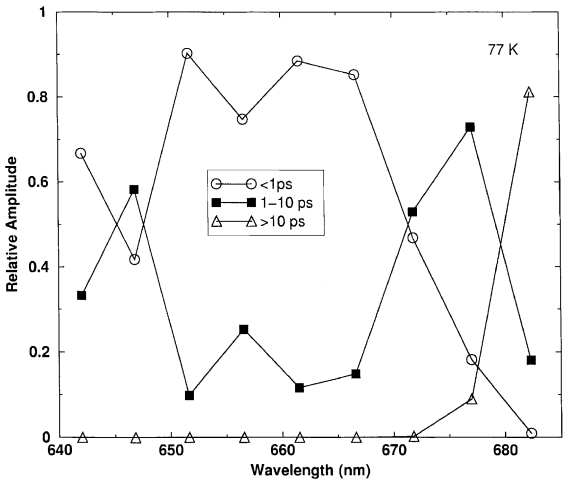

Fig. 12. Exciton life-times obtained at different wavelengths at 77 K for LHC-II monomers.

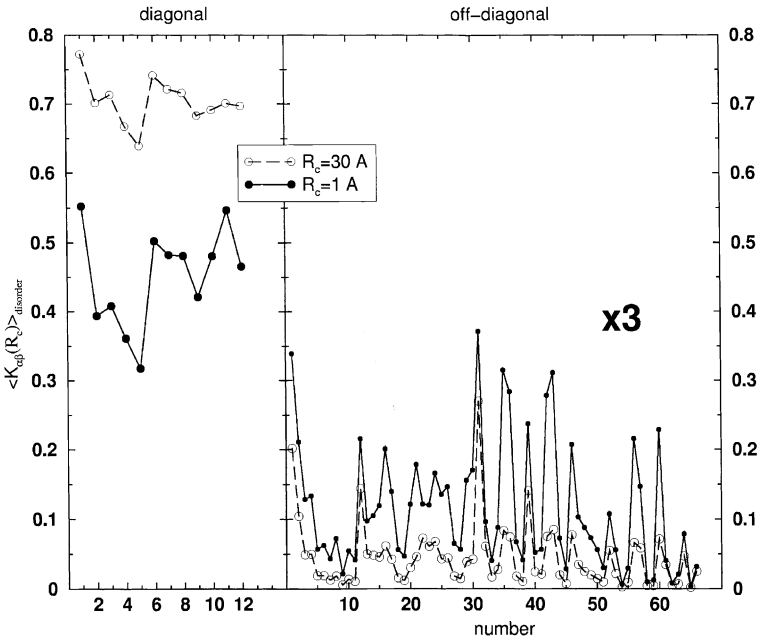

Fig. 13. Comparison of the diagonal elements of the exciton vibrational coupling with the off-diagonal coupling elements by means of the function $K_{\alpha\beta}(R_c)$ defined in Eq. (C.14) for two different values of the correlation radius $R_c = 1, 30$ Å. The x-axis on the left-hand side contains the number α of the exciton state, whereas the number on the x-axis on the right-hand side is a combination of the numbers α and β. The function $K_{\alpha\beta}(R_c)$ has been obtained from an average over 1000 randomly chosen configurations of disorder in site energies.

Fig. 12. A detailed comparison of theory and experiment would require to simulate the pump-probe spectra. Such a detailed simulation awaits, however, higher resolution structural data of the LHC-II complex.

5.3. Exciton–vibrational coupling

We want to finish with some more general considerations of the exciton–vibrational coupling in the LHC-II which might prove useful for the development of theory for the description of linear absorption spectra. The introduction of the function $K_{\alpha\beta}(R_c)$ in Eq. (C.12) makes it possible to compare the magnitudes of the off-diagonal elements of the exciton–vibrational coupling (contained in $K_{\alpha\alpha}$) with the magnitude of the diagonal elements (contained in $K_{\alpha\beta}$ for $\alpha \neq \beta$). In Fig. 13 the disorder averaged function $K_{\alpha\beta}(R_c)$ is shown for two different values of the correlation radius R_c. As is seen in this figure the off-diagonal elements are smaller by at least a factor of three. The reason of this difference lies in the different site energies assumed for the pigments and in the static disorder which both tend to localize the exciton wavefunction. This result provides a direct motivation for the introduction of excitonic potential energy surfaces and the perturbative treatment of the inter-PES coupling as it was done in Appendix B. We note that this theory allows to treat the diagonal part of the exciton vibrational coupling non-perturbatively.

6. Conclusion

To achieve a detailed understanding of chromophore complex absorption spectra the method of the reduced density operator combined with a time-dependent formulation of the absorption has been applied. Within this approach it could be shown that a certain approximation carried out with respect to the density operator equation is translated to an approximation of the absorption

coefficient. The obtained approximation accounts for the formation of delocalized exciton states as well as for the exciton–vibrational coupling. The usefulness of the approximation could be underlined in applying it to the pigment protein complex LHC-II of the light harvesting system belonging to the photosystem 2 of higher plants. And, we have been able to demonstrate for this example that a sufficient sophisticated computation of absorption spectra may lead one to interesting conclusions on the underlying microscopic structure. Furthermore, the density matrix approximation has been related to other descriptions of chromophore complex absorption spectra based on a systematic expansion with respect to vibrational satellites of increasing order.

The latter type of description has been used to investigate the influence of static and dynamic disorder on (compact) phenylacetylene dendrimers. Using static disorder of the site energies increasing from the inner to the outer part of the dendrimeric molecule measured absorption spectra could be reproduced in a satisfactory manner. Vibrational satellites have been also studied.

As an outlook we presented preliminary results on the computation of chromophore complex absorption spectra based on an exclusive expansion with respect to the part of the exciton vibrational coupling being off-diagonal with respect to the exciton quantum numbers. The obtained result looks promising and will be investigated in more detail in the near future.

Acknowledgements

This research was supported by the DFG through project Ma 1356/7. B. B. acknowledges it with thanks. T.R. would like to acknowledge support from the *Alexander von Humboldt Foundation* via a *Lynen Research Fellowship*.

Appendix A. Expansion with respect to the exciton–vibrational coupling

The expansion with respect to the whole coupling matrix $g_\xi(\alpha,\beta)$ represents a standard approach mainly used to compute vibrational satellites accompanying the basic (0–0) transition into the exciton levels. To have a compact notation of the whole perturbation series we split off the time-evolution operator in Eq. (2) (the dipole–dipole correlation function) into a free part and a part given by the exciton–vibrational coupling. The latter comprises the S-operator

$$S(t,0) = T\exp\left(-\frac{\mathrm{i}}{\hbar}\int_0^t \mathrm{d}\tau H^{(I)}_{\text{ex–vib}}(\tau)\right) \tag{A.1}$$

with the exciton–vibrational coupling in the interaction representation

$$H^{(I)}_{\text{ex–vib}}(\tau) = \sum_{\alpha,\beta} \mathrm{e}^{-\mathrm{i}\Omega_{\alpha\beta}\tau} \sum_\xi \hbar\omega_\xi g_\xi(\alpha\beta) Q_\xi(\tau)|\alpha\rangle\langle\beta|. \tag{A.2}$$

Note the abbreviation $\Omega_{\alpha\beta} = \Omega_\alpha - \Omega_\beta$ and the time-dependence of the Q_ξ originating from the vibrational Hamiltonian, Eq. (13). With the introduced S-operator the dipole–dipole correlation function, Eq. (2) is obtained as

$$C_{\text{d–d}}(t) = \sum_{\alpha\beta} \mathbf{d}^*_\alpha \mathbf{d}_\beta \mathrm{e}^{-\mathrm{i}\Omega_\alpha t} \mathrm{tr}_{\text{vib}}\{\hat{R}_{\text{eq}}\langle\alpha|S(t,0)|\beta\rangle\}, \tag{A.3}$$

including the vibrational equilibrium statistical operator $\hat{R}_{\text{eq}}$. Expanding the S-operator in powers of $H^{(I)}_{\text{ex–vib}}$ introduces vibrational satellites to the pure excitonic absorption spectrum. We do not give details here but refer to Section 3.1 where a somewhat more general approach including lifetime broadening of the exciton levels will be introduced.

The pure excitonic absorption spectrum, Eq. (5) is simply derived if one neglects any coupling to the vibrational DOF of the CC (approximation of a rigid CC). We neglect the related S-operator which reduces the trace in Eq. (A.3) to $\delta_{\alpha,\beta}$ and finally obtain the absorption coefficient according to Eq. (5). The absorption spectrum is given as a set of sharp lines corresponding to transitions into the various states of the exciton spectrum. Obviously this approach is disadvantegously from the conceptual point of view since any homogeneous line-broadening is absent. Furthermore, it is cumbersome task to carry out the perturbation

expansion of Eq. (A.3). As it is well known reasonable summations can only be obtained for the coupling of the exciton levels to a single (effective) vibrational mode. This difficulty is somewhat overcome if one uses the concept of excitonic PES, Eq. (15) to reformulate the perturbation formula, Eq. (A.3).

Appendix B. Expansion with respect to the off-diagonal part of the exciton–vibrational coupling

As mentioned at the end of Section 2 one can introduce PES which refer to the various exciton levels α and which are incorporated in the vibrational Hamiltonian, Eq. (15). Then, in similarity to the foregoing section it becomes possible to carry out an perturbation expansion with resect to the off-diagonal exciton–vibrational coupling. Now, instead of Eq. (A.3) we obtain (note the replacement of Ω_α by ε_α)

$$C_{\mathrm{d-d}}(t) = \sum_{\alpha\beta} \mathbf{d}_\alpha^* \mathbf{d}_\beta \mathrm{e}^{-\mathrm{i}\varepsilon_\alpha t} \times \mathrm{tr}_{\mathrm{vib}}\{\hat{R}_{\mathrm{eq}} U_0^+(t) U_\alpha(t) \langle\alpha|S(t,0)|\beta\rangle\}. \quad \text{(B.1)}$$

The time-evolution operator $U_0^+(t)$ has been defined by the ground-state CC Hamiltonian, Eq. (7) and we have set

$$U_\alpha(t) = \exp(-\mathrm{i}\Delta H_\alpha t/\hbar) \quad \text{(B.2)}$$

with $\Delta H_\alpha(Q)$ from Eq. (15). The S-operator reads

$$S(t,0) = T \exp\left(-\frac{\mathrm{i}}{\hbar} \int_0^t \mathrm{d}\tau \mathscr{H}^{(I)}_{\mathrm{ex-vib}}(\tau) \right). \quad \text{(B.3)}$$

It incorporates the off-diagonal part of the exciton–vibrational coupling (in the interaction representation)

$$\mathscr{H}^{(I)}_{\mathrm{ex-vib}}(\tau) = \sum_{\alpha\neq\beta} \mathrm{e}^{-\mathrm{i}\varepsilon_{\alpha\beta}\tau} \sum_\xi \hbar\omega_\xi g_\xi(\alpha\beta) U_\alpha^+ \times (\tau) Q_\xi(\tau) U_\beta(\tau) |\alpha\rangle\langle\beta|. \quad \text{(B.4)}$$

The time-dependence of the Q_ξ follows from the vibrational Hamiltonian, Eq. (13). Formula (B.1) gives the possibility to carry out a perturbational expansion with respect to the off-diagonal exciton–vibrational coupling. But a partial summation with respect to the diagonal part is already incorporated via the time-evolution operators defined by ΔH_α. Consequently, it would be of interest to study the case where the S-operator has been neglected in Eq. (B.1). It follows:

$$C_{\mathrm{d-d}}(t) = \sum_\alpha |\mathbf{d}_\alpha|^2 \mathrm{e}^{-\mathrm{i}\varepsilon_\alpha t} \mathrm{tr}_{\mathrm{vib}}\{\hat{R}_{\mathrm{eq}} U_0^+(t) U_\alpha(t)\}. \quad \text{(B.5)}$$

The trace with respect to the contributions of the excitonic PES reads

$$\mathrm{tr}_{\mathrm{vib}}\{\hat{R}_{\mathrm{eq}} U_0^+(t) U_\alpha(t)\} = \exp(-s_\alpha(0) + s_\alpha(t)), \quad \text{(B.6)}$$

where the line-shape function is given as

$$s_\alpha(t) \equiv s_{\alpha\alpha,\alpha\alpha}(t) = \int \mathrm{d}\omega \mathrm{e}^{-\mathrm{i}\omega t}(1+n(\omega))(J_{\alpha\alpha,\alpha\alpha}(\omega) - J_{\alpha\alpha,\alpha\alpha}(-\omega)). \quad \text{(B.7)}$$

The excitonic spectral density can be found in Appendix C. The absorption cross section follows as:

$$I(\omega) = \sum_\alpha |\mathbf{d}_\alpha|^2 \mathrm{e}^{-s_\alpha(0)} \int \mathrm{d}t \exp(\mathrm{i}(\omega - \varepsilon_\alpha)t + s_\alpha(t)). \quad \text{(B.8)}$$

This formula is similar to Eq. (3) but includes a partial summation with respect to the inter-chromophore Coulombic interaction and to all diagonal coupling matrix elements $g_\xi(\alpha,\alpha)$. Every excitonic level contributes independently from the other. But in contrast to the approximation of the rigid aggregate the absorption lines are broadened due to the inclusion of the vibrational DOF.

An expansion with respect to the off-diagonal exciton vibrational coupling is demonstrated in what follows. Although the concept of separating the exciton–vibrational coupling into a diagonal and off-diagonal part has been used elsewhere [46], it is not yet clear in the literature whether this approach is really useful or only represents a nice theoretical arabesque. In any case it has to be guaranteed that $g_\xi(\alpha,\alpha)\rangle|g_\xi(\alpha,\beta)|, \alpha \neq \beta$. That such a relation can be fulfilled is demonstrated for the CC of photosynthetic antenna systems in Section 5.

For the following the interaction between different PES will be treated in first-order perturbation theory leading to a separation of the correlation function according to

$$C_{\mathrm{d\text{–}d}}(\tau) = C^{(0)}_{\mathrm{d\text{–}d}}(\tau) + C^{(1)}_{\mathrm{d\text{–}d}}(\tau). \tag{B.9}$$

Here $C^{(0)}_{\mathrm{d\text{–}d}}$ is given in Eq. (B.5) and the first-order correction with respect to the off-diagonal exciton–vibrational coupling reads

$$C^{(1)}_{\mathrm{d\text{–}d}}(t) = -\mathrm{i}\sum_{\alpha\neq\beta}\int_0^t \mathrm{d}\tau \mathbf{d}^*_\alpha \mathbf{d}_\beta \mathrm{e}^{-\mathrm{i}\varepsilon_\alpha t}\mathrm{e}^{\mathrm{i}\varepsilon_{\alpha\beta}\tau} \times \mathrm{tr}_{\mathrm{vib}}\{\hat{R}_{\mathrm{eq}} U_0^+(t) U_\alpha(t-\tau)\Phi_{\alpha\beta}U_\beta(\tau)\}. \tag{B.10}$$

Note the abbreviation

$$\Phi_{\alpha\beta} = \sum_\xi \omega_\xi g_\xi(\alpha\beta) Q_\xi. \tag{B.11}$$

Introducing the displacement operator

$$D^+_\alpha = \exp\left\{\sum_\xi g_\xi(\alpha,\alpha)(C_\xi - C^+_\xi)\right\}, \tag{B.12}$$

we get the trace in Eq. (B.10) as

$$\mathrm{tr}_{\mathrm{vib}}\{\cdots\} = \mathrm{tr}_{\mathrm{vib}}\{\hat{R}_{\mathrm{eq}} U_0^+(t) D^+_\alpha U_0(t-\tau) \times D_\alpha \Phi_{\alpha\beta} D^+_\alpha D_\alpha D^+_\beta U_0(\tau) D_\beta\}. \tag{B.13}$$

Furthermore, it holds

$$D_j \Phi_{\alpha\beta} D^+_j = \Phi_{\alpha\beta} - 2\theta_{\alpha\beta}(j) \tag{B.14}$$

with the quantity

$$\theta_{\alpha\beta}(j) = \sum_\xi \omega_\xi g_\xi(\alpha,\beta) g_\xi(j,j), \tag{B.15}$$

resembling a reorganization energy. Next, we introduce the function [47]

$$F(\lambda) = -2\theta_{\alpha\beta}(\alpha)\mathrm{tr}_{\mathrm{vib}} \times \{\hat{R}_{\mathrm{eq}} D^+_\alpha(t) e^{-\lambda\Phi_{\alpha\beta}(\tau)/2\theta_{\alpha\beta}(\alpha)} D_{\alpha\beta}(\tau) D_\beta\} \tag{B.16}$$

which reduces to expression (B.13) when expanded with respect to λ up to linear terms and setting $\lambda = 1$. The time-dependence of the displacement operators has been defined according to

$$D_\alpha(t) = U_0^+(t) D_\alpha U_0(t) = \exp\left\{\sum_\xi g_\xi(\alpha,\alpha)(C_\xi \mathrm{e}^{-\mathrm{i}\omega_\xi t} - C^+_\xi \mathrm{e}^{\mathrm{i}\omega_\xi t})\right\} \tag{B.17}$$

and that of the coupling operator $\Phi_{\alpha\beta}$ in the same manner. The combined displacement operator $D_{\alpha\beta}$ is defined as $D_\alpha D^+_\beta$. The following properties of Bose operators are needed:

$$e^A e^B = \exp\left\{\sum_\xi (a_{1\xi} + a_{3\xi})C_\xi + (a_{2\xi} + a_{4\xi})C^+_\xi\right\} \times \exp\left\{\frac{1}{2}\sum_\xi (a_{1\xi}a_{4\xi} - a_{2\xi}a_{3\xi})\right\}, \tag{B.18}$$

where $A = \sum_\xi (a_{1\xi}C_\xi + a_{2\xi}C^+_\xi)$ and $B = \sum_\xi (a_{3\xi}C_\xi + a_{4\xi}C^+_\xi)$. A second-order cumulant expansion which is exact for harmonic oscillators gives for the thermal average

$$\mathrm{tr}_{\mathrm{vib}}\left\{\hat{R}_{\mathrm{eq}} \exp\left(\sum_\xi (a_{1\xi}C_\xi + a_{2\xi}C^+_\xi)\right)\right\} = \exp\left(\frac{1}{2}\sum_\xi a_{1\xi}a_{2\xi}(1 + 2n(\omega_\xi))\right), \tag{B.19}$$

where the Bose–Einstein distribution function of vibrational quanta $n(\omega)$ was introduced. By applying the above properties the correlation functions can be calculated. The first-order results for the absorption cross section reads

$$I^{(I)}(\omega) = \sum_{\alpha\neq\beta} \mathbf{d}^*_\alpha \mathbf{d}_\beta \mathrm{Im}\int_0^\infty \mathrm{d}t \int_0^t \mathrm{d}\tau \exp\{\mathrm{i}(\omega - \Omega_\beta)t - \mathrm{i}\Omega_{\alpha\beta}\tau + S_{\alpha\beta}(t,\tau) - S_{\alpha\beta}(0,0)\} \times (r_{\beta\beta,\beta\beta}(t-\tau) + r_{\alpha\beta,\alpha\alpha}(\tau) - E_{\alpha\beta}/\hbar). \tag{B.20}$$

The newly introduced functions read

$$S_{\alpha\beta}(t,\tau) = s_{\alpha\alpha,\beta\beta}(t) + s_{\beta\beta,\beta\beta}(t-\tau) - s_{\alpha\alpha,\beta\beta}(t-\tau) + s_{\alpha\alpha,\alpha\alpha}(\tau) - s_{\alpha\alpha,\beta\beta}(\tau), \tag{B.21}$$

where the line shape function has been introduced in Eq. (B.7). Furthermore, we defined

$$r_{\alpha\beta,j\delta}(t) = \int \mathrm{d}\omega \mathrm{e}^{-\mathrm{i}\omega t}(1 + n(\omega))(J_{\alpha\beta,j\delta}(\omega) + J_{\alpha\beta,j\delta}(-\omega)). \tag{B.22}$$

The quantity $E_{\alpha\beta}$ represents a certain form of a reorganization energy

$$E_{\alpha\beta} = \int \mathrm{d}\omega \hbar\omega (J_{\alpha\alpha,\alpha\beta}(\omega) + J_{\beta\beta,\alpha\beta}(\omega)). \tag{B.23}$$

This result demonstrates the general ability of the approach to give corrections proportional to powers of the off-diagonal exciton–vibrational coupling functions. Concrete numerical results will be given elsewhere.

Appendix C. The quantum master equation

To fix the notation we shortly quote the Quantum Master Equation (QME) which represents a non-Markovian equation of motion governing the reduced density operator. This type of density operator equation accounts for the coupling to the reservoir DOF in the second order of perturbation theory and represents the standard equation for all cases where the active system couples weakly or with intermediate strength to the reservoir (see, e.g. [48,49]). According to the notation of [2] it is written as

$$\begin{aligned}\frac{\partial}{\partial t}\hat{\rho}(t) = & -\frac{\mathrm{i}}{\hbar}(H_{\mathrm{S}},\hat{\rho}(t))_- \\ & -\sum_{u,v}\int_0^{t-t_0}\mathrm{d}\tau\{C_{uv}(\tau)(K_u,U_{\mathrm{S}}(\tau)K_v \\ & \times\hat{\rho}(t-\tau)U_{\mathrm{S}}^{+}(\tau))_- - C_{vu}(\tau)(K_u,U_{\mathrm{S}}(\tau) \\ & \times\hat{\rho}(t-\tau)K_v U_{\mathrm{S}}^{+}(\tau))_-\}. \end{aligned} \tag{C.1}$$

H_{S} has to be understood as the Hamiltonian of the active system, and the system–reservoir coupling has been used in the general form

$$H_{\mathrm{S\text{–}R}} = \hbar\sum_u K_u\Phi_u, \tag{C.2}$$

with operators K_u and Φ_u acting exclusively in the state-space of system and reservoir states, respectively. The correlation function in Eq. (C.1) is the equilibrium correlation of the reservoir DOF, i.e.,

$$C_{uv}(\tau) = \mathrm{tr}_{\mathrm{R}}\{\hat{R}_{\mathrm{eq}}\mathrm{e}^{\mathrm{i}H_{\mathrm{R}}\tau/\hbar}\Phi_u(\tau)\mathrm{e}^{-\mathrm{i}H_{\mathrm{R}}\tau/\hbar}\Phi_v\}. \tag{C.3}$$

Here we identify the active-system Hamiltonian by the electronic ground-state of the CC (with projection operator $\hat{P}_0$) and the exciton states (with projection operator $\hat{P}_1$). Therefore, we write $H_{\mathrm{S}} = E_0P_0 + H_{\mathrm{ex}}P_1$ (compare Eq. (6), a generalization including high-frequency vibrational DOF has been given in Section 3.2). As already noted the ground-state energy E_0 is set equal to zero. The system–reservoir coupling $H_{\mathrm{S\text{–}R}}$ has to be identified with the exciton–vibrational interaction, Eq. (11) restricted to the excited states. Hence, we can identify the index u with the pair $\alpha\beta$ and have

$$K_{\alpha\beta} = |\alpha\rangle\langle\beta| \equiv K_{\alpha\beta}\hat{P}_1 \tag{C.4}$$

and

$$\Phi_{\alpha\beta} = \sum_\xi \omega_\xi g_\xi(\alpha\beta)Q_\xi. \tag{C.5}$$

If the vibrational DOF are described by independent harmonic oscillators the correlation function, Eq. (C.3) can be written as

$$\begin{aligned}C_{\alpha\beta j\delta}(t) = & \int \mathrm{d}\omega\mathrm{e}^{-\mathrm{i}\omega t}\omega^2(1+n(\omega))(J_{\alpha\beta,j\delta}(\omega) \\ & - J_{\alpha\beta,j\delta}(-\omega)), \end{aligned} \tag{C.6}$$

where the spectral density is defined as

$$J_{\alpha\beta,j\delta}(\omega) = \sum_\xi g_\xi(\alpha,\beta)g_\xi(j,\delta)\delta(\omega-\omega_\xi). \tag{C.7}$$

The frequency dependent correlation function $C_{\alpha\beta j\delta}(\omega)$ can be directly deduced from Eq. (C.6), whereas the half-sided Fourier-transform $\tilde{C}$ can be obtained from

$$\tilde{C}_{\alpha\beta j\delta}(\omega) = -\int\frac{\mathrm{d}\bar{\omega}}{2\pi\mathrm{i}}\frac{C_{\alpha\beta j\delta}(\bar{\omega})}{\omega-\bar{\omega}+\mathrm{i}\varepsilon}. \tag{C.8}$$

The real part simply follows as:

$$\begin{aligned}\mathrm{Re}\tilde{C}_{\alpha\beta,\beta\alpha}(\omega) = & \pi\omega^2(1+n(\omega))(J_{\alpha\beta\beta\alpha}(\omega) \\ & - J_{\alpha\beta\beta\alpha}(-\omega)) \end{aligned} \tag{C.9}$$

and the imaginary part can be deduced from the real part via a Kramers–Kronig like relation

$$\mathrm{Im}\tilde{C}_{\alpha\beta,\beta\alpha}(\omega) = \frac{1}{\pi}\mathscr{P}\int\mathrm{d}\bar{\omega}\frac{\mathrm{Re}C_{\alpha\beta,\beta\alpha}(\bar{\omega})}{\omega-\bar{\omega}}. \tag{C.10}$$

The spectral density $J_{\alpha\beta\beta\alpha}(\omega)$, Eq. (C.7) is related to the local exciton–vibrational coupling via the local representation of the excitonic coupling constants $g_\xi(\alpha,\beta)$ (see, Eq. (12))

$$\begin{aligned}J_{\alpha\beta\beta\alpha}(\omega) = & \sum_{m,n}C_\alpha^*(m)C_\beta(m)C_\beta^*(n)C_\alpha(n) \\ & \times\sum_\xi g_\xi^2(m)g_\xi^2(n)\delta(\omega-\omega_\xi). \end{aligned} \tag{C.11}$$

If one introduces a correlation radius of the vibrational degrees of freedom as it was done in [18]

the above expression for the spectral density can be simplified to

$$J_{\alpha\beta\beta\alpha}(\omega) = K_{\alpha\beta}(R_c)J(\omega). \tag{C.12}$$

Here a local spectral density $J(\omega)$ was introduced as

$$J(\omega) = \sum_{\xi} g_{\xi}^2 \delta(\omega - \omega_{\xi}), \tag{C.13}$$

common to all sites (chromophores) in the CC. The function

$$K_{\alpha\beta}(R_c) = \sum_{m,n} C_{\alpha}^*(m)C_{\beta}(m)C_{\beta}^*(n)C_{\alpha}(n)e^{-R_{mn}/R_c} \tag{C.14}$$

contains the exciton coefficients, the correlation radius R_c of the vibrational degrees of freedom as well as the inter-chromophore distances R_{mn}.

Since the density operator being of interest here is off-diagonal, i.e., is given as the coherence between the electronic ground-state and the first excited electronic CC-state we can simplify the QME, Eq. (C.1) to get

$$\begin{aligned}\frac{\partial}{\partial t}\hat{P}_1\hat{\rho}(t)\hat{P}_0 = & -\frac{i}{\hbar}(H_1\hat{P}_1\hat{\rho}(t)\hat{P}_0 - \hat{P}_1\hat{\rho}(t)\hat{P}_0H_0) \\ & - \sum_{u,v}\int_0^{t-t_0} d\tau C_{uv}(\tau)K_uU_1(\tau)K_v\hat{P}_1 \\ & \times \hat{\rho}(t-\tau)\hat{P}_0U_0^+(\tau).\end{aligned} \tag{C.15}$$

Changing to the (off-diagonal) matrix elements

$$\rho_{\alpha 0}(t) = \langle\alpha|\hat{\rho}(t)|0\rangle \tag{C.16}$$

it follows:

$$\begin{aligned}\frac{\partial}{\partial t}\rho_{\alpha 0}(t) = & -i\Omega_{\alpha}\rho_{\alpha 0}(t) \\ & - \sum_{\beta,j}\int_0^{t-t_0} d\tau e^{-i\Omega_{\beta}\tau}C_{\alpha\beta\beta j}(\tau)\rho_{j0}(t-\tau).\end{aligned} \tag{C.17}$$

Obviously, $\rho_{\alpha 0}$ can be identified with the quantity B_{α}, Eq. (21). The dissipative part reduces to simple dephasing if one neglects contributions with $j \neq \alpha$ and carries out the Markov limits. To this end one replaces $\rho_{\alpha 0}(t-\tau)$ by $\exp(i\Omega_{\alpha}\tau)\rho_{\alpha 0}(t)$ and extends the time-integral up to infinity. It follows:

$$\left(\frac{\partial\rho_{\alpha 0}(t)}{\partial t}\right)_{diss} = -\Gamma_{\alpha}\rho_{\alpha 0}(t), \tag{C.18}$$

where the dephasing rate reads

$$\begin{aligned}\Gamma_{\alpha} = \pi\sum_{\beta}\Omega_{\alpha\beta}^2\big((1+n(\Omega_{\alpha\beta}))J_{\alpha\beta,\beta\alpha}(\Omega_{\alpha\beta}) \\ + n(\Omega_{\beta\alpha})J_{\alpha\beta,\beta\alpha}(\Omega_{\beta\alpha})\big).\end{aligned} \tag{C.19}$$

References

[1] S. Mukamel, Principles of Nonlinear Optical Spectroscopy, Oxford, New York, 1995.
[2] V. May, O. Kühn, Charge and Energy Transfer Dynamics in Molecular Systems, Wiley/VCH, Berlin, 1999.
[3] A.S. Davydov, Theory of Molecular Excitons, Plenum Press, New York, 1971.
[4] A. Suna, Phys. Rev. 135 (1964) A111.
[5] M.R. Philpott, J. Chem. Phys. 47 (1967) 2534.
[6] J. Klafter, J. Jortner, J. Chem. Phys. 68 (1978) 1531.
[7] E.W. Knapp, Chem. Phys. 85 (1984) 73.
[8] N. Lu, S. Mukamel, J. Chem. Phys. 95 (1991) 1588.
[9] H. Fidder, J. Knoester, D.A. Wiersma, J. Chem. Phys. 95 (1991) 7880.
[10] C. Warns, I. Barvik, P. Reineker, T. Neidlinger, Chem. Phys. 194 (1995) 117.
[11] L.D. Bakalis, M. Coca, J. Knoester, J. Chem. Phys. 110 (1999) 2208.
[12] D.V. Makhov, V.V. Egorov, A.A. Bagatr'yants, M.V. Alfimov, J. Chem. Phys. 110 (1999) 3196.
[13] R. Scheller, V. May, Chem. Phys. 264 (1999) 191.
[14] V.A. Malyshev, A. Rodriguez, F. Dominguez-Adame, Phys. Rev. B 60 (1999) 14140.
[15] F. Dominguez-Adame, V.A. Malyshev, A. Rodriguez, J. Phys. Chem. 112 (2000) 3023.
[16] O. Kühn, V. Sundström, J. Phys. Chem. B 101 (1997) 3432.
[17] O. Kühn, V. Sundström, J. Chem. Phys. 107 (1997) 4154.
[18] Th. Renger, V. May, J. Phys. Chem. A 102 (1998) 4381.
[19] O. Kühn, T. Renger, V. May, J. Voigt, T. Pullerits, V. Sundström, Trends Photochem. Photobiol. 4 (1997) 213.
[20] Th. Renger, V. May, O. Kühn, Phys. Rep. 343 (2001) 137.
[21] R. Kopelman, M. Shortreed, Z.-Y. Shi, W. Tan, Z. Xu, J.S. Moore, A. Bar-Haim, J. Klafter, Phys. Rev. Lett. 78 (1997) 1239.
[22] F. Neugebauer, V. May, Chem. Phys. Lett. 289 (1998) 67.
[23] Such a replacement becomes only possible by incorporating the high-frequency vibrational DOF into the active system. If one uses the original equation of motion 23 and splits off the correlation function $C_{\alpha\beta,\beta j}$ into a part formed by the high-frequency and a one by the low-frequency vibrational DOF such a replacement does not work. One is only able to replace Ω_{α} by $\Omega_{\alpha} - i\Gamma_{\alpha}$ in the first term on the right-hand side of Eq. (23)..
[24] Z. Xu, M. Kahr, K.L. Walker, Ch.L. Wilkins, J.S. Moore, J. Am. Chem. Soc. 116 (1994) 4537.
[25] Ch. Devadoss, P. Bharathi, J.S. Moore, J. Am. Chem. Soc. 118 (1996) 9635.

[26] A. Bar-Haim, J. Klafter, J. Lum. 76 & 77 (1998) 197.
[27] S.F. Swallen, Z.-Y. Shi, W. Tan, Z. Xu, J.S. Moore, R. Kopelman, J. Lum. 76 & 77 (1998) 193.
[28] J.C. Kirkwood, Ch. Scheurer, V. Chernyak, S. Mukamel, J. Chem. Phys. 114 (2001) 2419.
[29] S. Tretiak, V. Chernyak, Sh. Mukamel, J. Phys. Chem. B 102 (1998) 3310.
[30] E.Y. Poliakov, V. Chernyak, S. Tretiak, S. Mukamel, J. Chem. Phys. 110 (1999) 8161.
[31] V. Chernyak, E.Y. Poliakov, S. Tretiak, S. Mukamel, J. Chem. Phys. 111 (1999) 4158.
[32] S. Raychaudhuri, Y. Shapir, V. Chernyak, S. Mukamel, Phys. Rev. Lett. 85 (2000) 282.
[33] R. van Grondelle, J.P. Dekker, T. Gillbro, V. Sundström, Biochim. Biophys. Acta 1187 (1994) 1.
[34] P.W. Hemelrijk, S.L.S. Kwa, R. van Grondelle, J.P. Dekker, Biochim. Biophys. Acta 1098 (1992) 159.
[35] J. Voigt, Th. Renger, R. Schödel, J. Pieper, H. Redlin, Phys. Stat. Sol. 194 (1996) 333.
[36] H. van Amerongen, R. van Grondelle, J. Phys. Chem. B 105 (2001) 604.
[37] W. Kühlbrandt, D.N. Wang, Y. Fujiyoshi, Nature 367 (1994) 614.
[38] R. Remelli, C. Varotto, D. Sandona, R. Groce, R. Bassi, J. Biol. Chem. 274 (1999) 33510.
[39] H. Rogl, W. Kühlbrandt, Biochemistry 38 (1999) 16214.
[40] D. Gülen, R. van Grondelle, H. van Amerongen, J. Phys. Chem. 101 (1997) 7256.
[41] C.C. Gradinaru, S. Özdemir, D. Gülen, I.H.M. Stokkum, R. van Grondelle, H. van Amerongen, Biophys. J. 75 (1998) 3046.
[42] Th. Renger, V. May, Phys. Rev. Lett. 84 (2000) 5228.
[43] The optimization procedure was organized in the following way. For each dipole configuration a set of several hundred randomly chosen start simplexes were optimized in the high-dimensional parameter space by minimizing the sum over squared deviations between experimental and simulation data. Finally the best optimized subsets of the different geometries were compared. The two chosen optimal dipole geometries gave an about 50% smaller least square function than the remaining geometries. For a description of the Simplex algorithm see W.H. Press et al., Numerical Recipes in Fortran, Cambridge University Press, Cambridge, 1992.
[44] J. Pieper, M. Rätsep, R. Jankowiak, K.D. Irrgang, J. Voigt, G. Renger, G.J. Small, J. Phys. Chem. A 103 (1999) 2412.
[45] H.M. Visser, F.J. Kleima, I.H.M. van Stokkum, R. van Grondelle, H. van Amerongen, Chem. Phys. 210 (1996) 297.
[46] V. Chernyak, W.M. Zhang, S. Mukamel, J. Chem. Phys. 109 (1998) 9587.
[47] C.K. Chan, J. Chem. Phys. 81 (1984) 1614.
[48] R. Kubo, M. Toda, N. Hashitsume, Statistical Physics II: Nonequilibrium Statistical Mechanics, Springer, Berlin, 1985.
[49] K. Blum, Density Matrix Theory and Applications, Plenum Press, New York, 1996.
[50] J. Voigt, Th. Schrötter, Z. Phys. Chem. Part 2 211 (1999) 181.
[51] S. Nussberger, J.P. Decker, W. Kühlbrandt, B.M. van Bolhuis, R. van Grondelle, H. van Ameronge, Biochemistry 33 (1994) 14775.